PROPOSAL FOR 50 GEV PROTON SYNCHROTRON

# Search for H-Dibaryon with a Large Acceptance Hyperon Spectrometer


J.K. Ahn (*spokesperson*), S.H. Hwang, S.H. Kim,
S.J. Kim, S.Y. Kim, A. Ni, J.Y. Park, S.Y. Ryu
*Pusan National University, Korea*

S. Hasegawa, R. Honda, Y. Ichikawa, K. Imai (*co-spokesperson*),
H. Sako, S. Sato, K. Shirotori, H. Sugimura
*Japan Atomic Energy Agency (JAEA), Japan*

H. Fujioka, M. Niiyama
*Kyoto University, Japan*

R. Kiuchi, K. Tanida
*Seoul National University, Korea*

M. Ieiri, K. Ozawa, H. Takahashi, T. Takahashi
*High Energy Accelerator Research Organization (KEK), Japan*

K. Nakazawa, M. Sumihama
*Gifu University, Japan*

B. Bassalleck
*University of New Mexico, USA*



December 10, 2011

# Abstract

Recent Lattice QCD calculation, which succeeded to reproduce nucleon-nucleon potential, has been extended to baryon-baryon interactions in $\mathrm{SU_f}(3)$ symmetry (for pion masses still off the physical value). The HAL collaboration has shown no repulsive core but attractive potential at a short distance in the baryon-baryon interaction in the $\mathrm{SU_f}(3)$ singlet state, namely H-dibaryon channel. They suggest the H-dibaryon may appear as a weakly bound state or a resonant state near the $\Lambda\Lambda$ threshold. The NPLQCD collaboration found the bound H-dibaryon in LQCD calculation without $\mathrm{SU_f}(3)$ symmetry and also suggests the H-dibaryon around the threshold. We propose to search for the H-dibaryon resonance in $\Lambda\Lambda$ production from $(K^-, K^+)$ reactions off nuclei and the bound H-dibaryon by its weak decays to answer the long-standing question about the existence of the H-dibaryon. Being able to simultaneously search below and above threshold is a unique and novel feature of this proposal. For this experiment, we propose to construct a large acceptance hyperon spectrometer with a Time Projection Chamber (TPC) to detect $\Lambda$ particles with high statistics and an excellent energy resolution. This spectrometer will also enhance the capability of hadron physics at J-PARC.

# 1 Physics Motivation

Many Quantum Chromodynamics (QCD) theories predict that there should be a possibly bound H-dibaryon, which has a $uuddss$ quark configuration $(I = J = 0)$ of maximal spatial symmetry. There has been as yet no definitive observation of the stable H-dibaryon, despite strenuous experimental efforts using a variety of approaches since the first theoretical prediction by R. Jaffe [1, 2]. The observation of double $\Lambda$ hypernuclei implies a lower limit of the mass of the H-dibaryon [3]. The most stringent lower limit is about 7 MeV below the $\Lambda\Lambda$ threshold determined by the mass of a ${}_{\Lambda\Lambda}^{6}$He, albeit based on only one event in emulsion plates exposed to a 1.67-GeV$/c$ $K^-$ beam in the KEK-E373 hybrid-emulsion experiment [4].

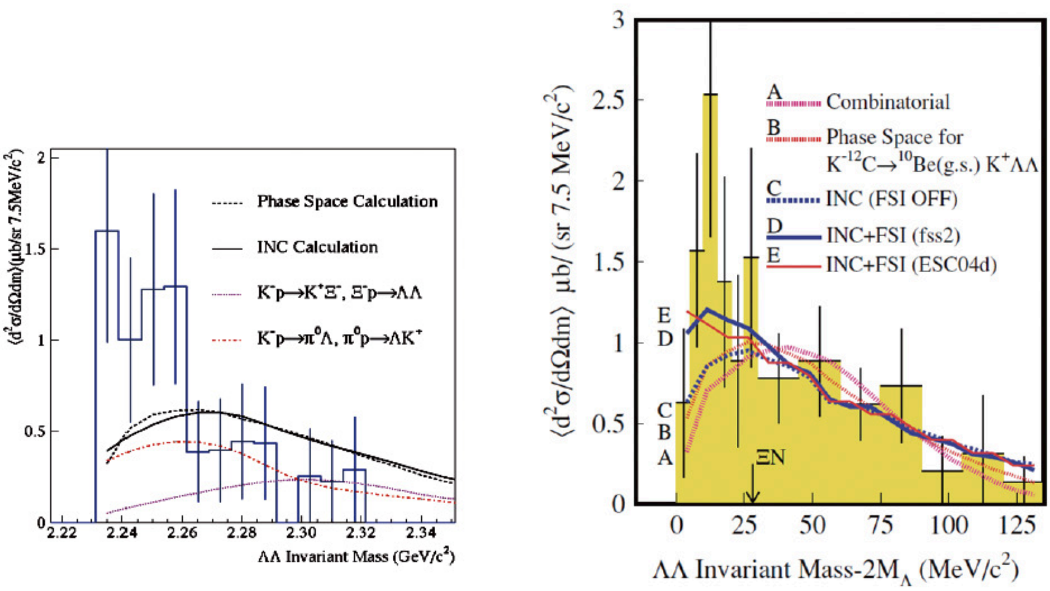


(a) (b)

Figure 1: (a) $\Lambda\Lambda$ invariant mass spectrum (E224) with overlaid lines for the 3-body phase space and intra-nuclear cascade calculation results. Enhanced $\Lambda\Lambda$ production near the threshold beyond the level predicted with known two-step processes has been observed [5] ; (b) $\Lambda\Lambda$ invariant mass spectrum (E522) is compared to calculations, phase space (A), intra-nuclear cascade (INC) calculations without final state interaction (B) and with final state interactions (C,D). Although a peak structure is found at 2242 MeV/c$^2$, the data also favor final state interactions within statistical errors [6].

While experimental searches for an unbound H-dibaryon have yielded no conclusive evidence in high-energy experiments, a KEK experiment (E224) has reported enhanced $\Lambda\Lambda$ production near the $\Lambda\Lambda$ threshold in the $^{12}$C$(K^-, K^+)$ reaction with a scintillating-fiber active target [5], which was reconfirmed in a later KEK experiment (E522) with a relatively larger statistics due to a larger target volume [6], as shown in Fig 1a and 1b, respectively. The enhancement is then suggestive of either the possible existence of an H-dibaryon resonance with the mass of 2242 MeV$/c^2$, just 12 MeV$/c^2$ above the threshold, or a strongly-attractive $\Lambda\Lambda$

final-state interaction, or both. Due to limited statistics, however, it is difficult to draw a definite conclusion whether there exists the H-dibaryon resonance or not near the $\Lambda\Lambda$ threshold.

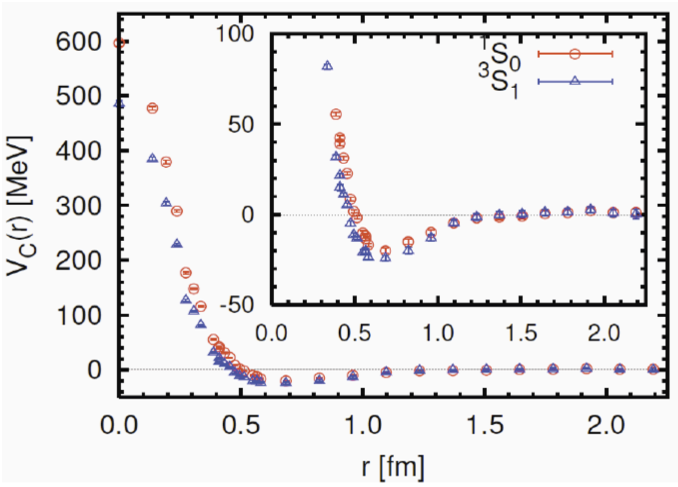


Figure 2: The Lattice QCD result on the nucleon-nucleon potential that is reproduced qualitatively from the first principle by Ishii, Aoki and Hatsuda [7].

Recent Lattice QCD calculations have had great success in reproducing the properties of the nucleon-nucleon interaction [7]. The nuclear force, attractive potential at long distance and short range repulsion, was reproduced by the first principle calculation for the first time as shown in Fig. 2. The HAL collaboration extended this Lattice QCD calculation to the baryon-baryon interactions under $\mathrm{SU_f}(3)$ symmetry [8]. Very recently, they published the result on the two-body potential for the singlet state, namely the H-dibaryon state [9]. Fig. 3 shows the obtained potential which shows no repulsive core but a strongly attractive potential at a short distance. The result is stable against the lattice sizes from 2 to 4 fm. Although the Lattice QCD calculations are still for pion masses far off the physical value (from 1015 to 673 MeV), the mass dependence seems to be weak. This striking result is qualitatively consistent with various quark model calculations based on the color-magnetic interaction and generalized Pauli principle among quarks. From this potential the H-dibaryon appears as a bound state by $\mathrm{B_H} = 35.6 \pm 7.4 \pm 4.0$ MeV at the pion mass of 673 MeV. This result was obtained under $\mathrm{SU_f}(3)$ symmetry.

The H-dibayon state can be written with known hyperons as follows,

$$H = -\sqrt{1/8}\Lambda\Lambda + \sqrt{3/8}\Sigma\Sigma + \sqrt{4/8}\Xi N \tag{1}$$

In the real world of $\mathrm{SU_f}(3)$ breaking, the quoted binding energy $\mathrm{B}_H$ can be then interpreted as the binding energy from the average mass of two octet baryons. Inoue *et al.* [9] pointed out that the difference between the average mass and 2 $\Lambda$ mass is close to $\mathrm{B}_H$, so the H-dibaryon may appear as a weakly bound state or a resonant state near $\Lambda\Lambda$ threshold.

The NPLQCD collaboration performed the Lattice QCD calculation using Luscher's finite-volume method without $\mathrm{SU_f}(3)$ symmetry ($n_\mathrm{f} = 2 + 1$). They have found that the H-dibaryon

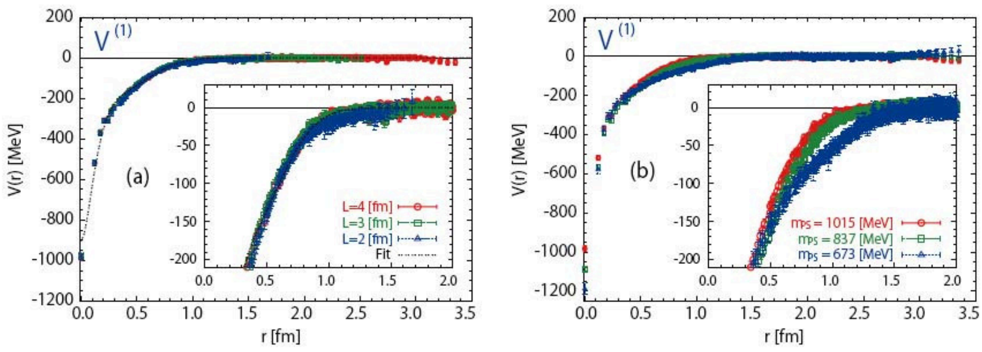


Figure 3: The BB potential in the $SU_f(3)$ singlet state calculated with Lattice QCD by HAL collaboration [8]. There is no repulsive core in this H-channel. (a) shows the lattice size dependence from 2 to 4 fm and (b) shows pion mass dependence from 673 to 1015 MeV.

is bound with the binding energy of $B_H = 16.6 \pm 2.1 \pm 4.5$ MeV at even smaller pion mass of 389 MeV [10]. They discussed the extrapolation of the $B_H$ to the physical value with both HAL and NPLQCD results, and concluded that the H-dibaryon should exist around the $\Lambda\Lambda$ threshold [11] (see Fig.4). Shanahan, Thomas and Young studied the chiral extrapolation from these LQCD results to the physical point and claimed that the H mass is 13 ± 14 MeV above the $\Lambda\Lambda$ threshold [22].

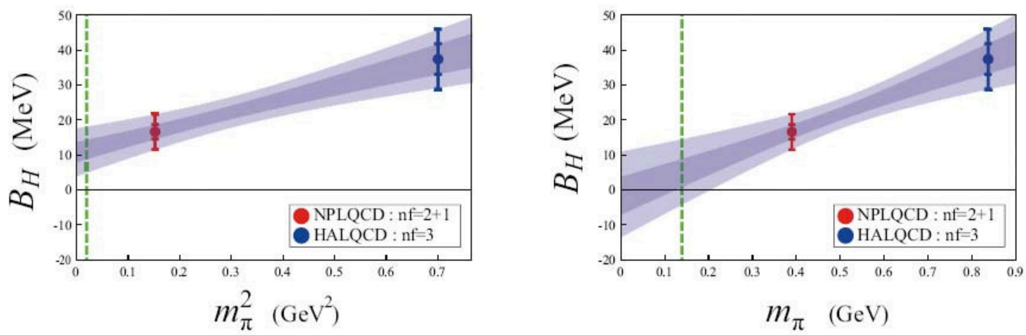


Figure 4: The results of Lattice QCD calculations on the H-dibaryon from the HAL collaboration (blue circle) and the NPLQCD collaboration (red circle). Shaded regions correspond to an extrapolation of the LQCD results with quadratic (left) and linear (right) functions of $m_\pi^2$, respectively, to the physical mass point (green dashed line).

Recent measurement of a two-solar-mass neutron star has attracted much attention [20]. The mass was calculated to be 1.97 ± 0.04 solar-mass using Shapiro delay, which rules out almost all currently proposed hyperon or boson condensate equations of state. It is claimed that quark matter (strange quark matter) at the core of neutron star can support such a massive star [20]. The H-dibaryon is regarded as a lightest strange quark matter, so it provides a doorway to explore possible strange quark matter in neutron stars.

Considering the Lattice QCD calculation results and the previous experimental results (KEK-E224 and E522) with a hint on a possible H-dibaryon resonance, we believe it is very important to experimentally answer the long-standing question about the existence of the H-dibaryon.

We propose to measure the same $\Lambda\Lambda$ production off nuclei in $(K^-, K^+)$ reaction using a high-intensity $K^-$ beam at J-PARC. To obtain much higher statistics and better mass resolution, we propose to construct a large-acceptance hyperon spectrometer with a Time Projection Chamber (TPC). We expect to collect 3300 $\Lambda\Lambda$ events with a mass resolution of 1.0 MeV for 100 shifts. The previous KEK-PS E522 experiment observed about 90 events with a mass resolution of 5 MeV. The TPC enables us to search for the weakly-bound H-dibaryon decaying to $\Sigma^- p$ and $\Lambda p\pi^-$ in-flight as well.

# 2 Experiment

## 2.1 The goal of the proposed experiment

The first goal of the experiment is to conclude whether the previously observed enhancement near the $\Lambda\Lambda$ threshold is due to the existence of the H-resonance or not. The observed enhancement provided the central value of the mass (2250 MeV) and the production cross section of about $1\mu$b/sr for the possible H-resonance. With the proposed experimental apparatus we simulated $\Lambda\Lambda$ production assuming that the production yield of the H-dibaryon resonance is of the same order of the observed enhancement. The simulated $\Lambda\Lambda$ invariant-mass spectrum was shown in Fig.5, where the momentum resolution ($\Delta p/p$) of decay particles from the $\Lambda$ decay is assumed to be 3% at $p = 300$ MeV$/c$ and the intrinsic H width is assumed to be zero in the simulation. Experimental details will be described in the following section.

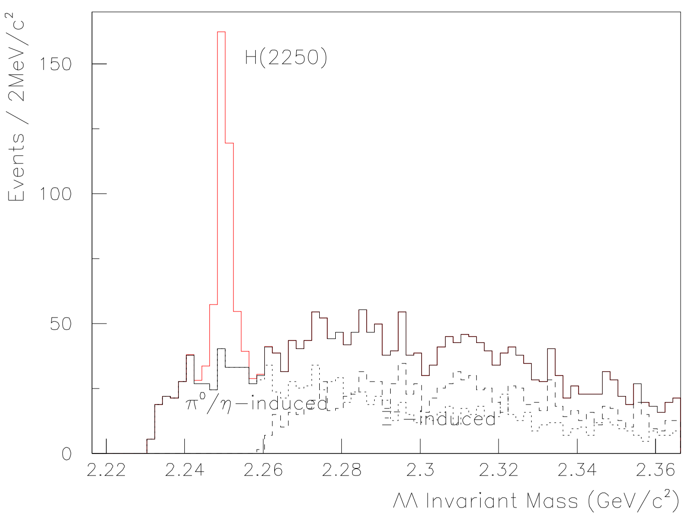


Figure 5: Simulated $\Lambda\Lambda$ invariant spectrum expected in the proposed experiment assuming the H-dibaryon resonance ($m = 2250$ MeV$/c^2$ and $\Gamma = 0$ MeV) produced with the production yield corresponding to the peak structure observed in the previous experiment. The peak width is then determined by detector resolutions.

The second goal is to provide more stringent upper limit for the production of H-dibaryon. Many experimental results ruled out the H-dibaryon up to the mass of about 2200 MeV$/c^2$ [12] as shown in Fig.6. The dashed and dotted lines indicate the theoretical calculation results predicted by Aerts and Dover [13] with different choices for elementary $p(K^-, K^+)\Xi^-$ reaction cross-section, respectively. However, there has been no successful experimental approach to explore the H-dibaryon mass range near the $\Lambda\Lambda$ threshold because of a large tail of quasi-free $\Xi^-$ production and other processes.

We are then in a position to explore the existence of the H-dibaryon assuming the production cross section of about $0.2\mu$b/sr for $^3$He target by Aerts and Dover [13]. The simulated

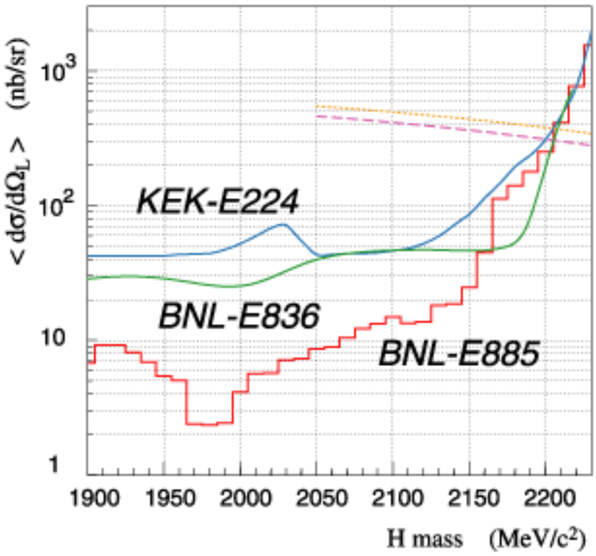


Figure 6: The 90% C.L. upper limits on the direct H-dibaryon production cross sections on $^{12}$C (BNL-E885), shown together with the upper limits obtained in E224 and E836 ($^{3}$He target). The dashed and dotted lines show the theoretical calculations by Aerts and Dover for $^{12}$C with different choices for elementary $p(K^-, K^+)\Xi^-$ reaction cross-section, respectively. The upper limits are similar to the calculations at around 2210 MeV.

$\Lambda\Lambda$ spectrum is shown in Fig.7 with the same cross section for Cu as for $^{3}$He (0.2 $\mu$b/sr). The cross section for the Cu target is expected to be much larger than $^{3}$He (The number of relative $S$-wave pp pairs is calculated to be $0.13A^{1.44}$ [14], thereby yielding the ratio of Cu to $^{3}$He to be about 50.)

There still remains a possibility to search for the weakly-bound H-dibaryon by less than 7 MeV below the $\Lambda\Lambda$ threshold. In this case, it decays weakly to $\Lambda n$, $\Sigma^- p$, $\Sigma^0 n$ and $\Lambda p \pi^-$ in flight. Among them, $\Sigma^- p$ and $\Lambda\pi^- p$ decays can be detected with the proposed experimental setup. These decay modes were actually searched for with a scintillating fiber active target in E224. Null result yielded an upper limit on the production cross section to be 0.6 $\sim$ 0.7 % of quasi-free $\Xi^-$ production cross section [15]. However, the scintillating-fiber detector has limited sensitivity to the $H \rightarrow \Sigma^- p$ decay since secondary interactions such as $\Lambda + (n) \rightarrow \Sigma^- p$ show a similar event pattern. Detection sensitivity depends significantly on the mean lifetime of the H dibaryon due to the limited size ($10 \times 10 \times 10$ cm$^3$). While the E224 scintillating-fiber detector has reasonable sensitivity to detect the H with mean lifetime of hyperons, it has very limited sensitivity for the 10-times longer-lived H than hyperons as suggested by J.F. Donoghue *et al.* [18], The proposed experiment has 100 times higher sensitivity than E224 because of higher $K^-$ beam intensity and much less secondary interaction of a gas detector. It has also a sufficient sensitivity for such a very long-lived H because of a larger size of

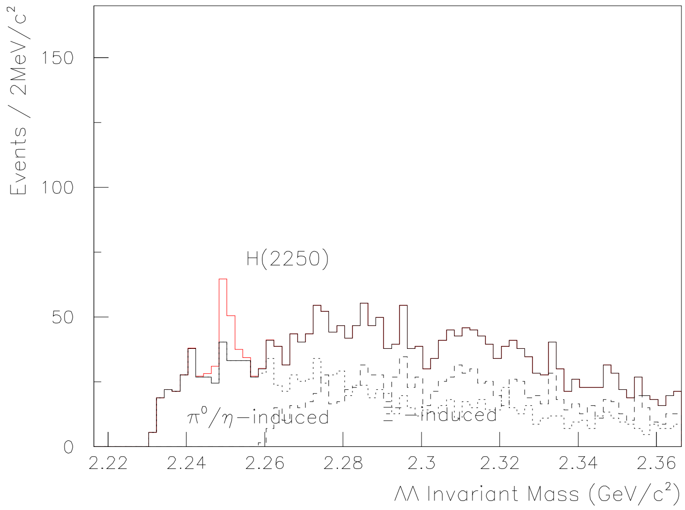


Figure 7: The result of the simulation for $\Lambda\Lambda$ invariant spectrum expected in the proposed experiment, if the H-dibaryon resonance is produced with the cross section of 0.2 $\mu$b/sr predicted by A. Aerts and C. Dover [12]. The cross section for the Cu target is expected to be much larger than $^3$He.

the detector. In the simulation the 2220 MeV/$c^2$ H-dibaryon (just below the threshold) are produced via the $(K^-, K^+)$ reaction and decays to $\Lambda\pi^- p$ in-flight, as shown in Fig.8. The background accounts for misidentified $\Lambda\Lambda$ events as $\Lambda p\pi^-$ events.

We are also able to explore information on the scattering length of $\Lambda\Lambda$ interaction in the proposed experiment. By applying a method on dispersion theory to the $\Lambda\Lambda$ invariant spectrum obtained from E522, A.M. Gasparyan *et al.* deduced a $^1$S$_0$ scattering length of $a_{\Lambda\Lambda} = -1.2 \pm 0.6$ fm [21]. The proposed measurement will measure the $\Lambda\Lambda$ scattering length with much higher precision. With the hyperon spectrometer, one can measure $\Xi^-$ momentum in correlation with $K^+$ momentum. The $\Xi^-$ hyperon produced inside a nucleus is affected by the $\Xi^-$-nucleus potential. The measurement of the $\Xi^-$ momentum distribution from nuclei, which has never been performed so far, will provide information on the $\Xi^-$-nucleus potential.

## 2.2 Experimental setup

We will measure $(K^-, K^+)$ reaction off nuclei with use of the 1.8 GeV/c $K^-$ beam at J-PARC and the Kurama $K^+$ spectrometer. In addition, we will construct a large acceptance hyperon spectrometer with TPC to detect $\Lambda$ particles to search for the H-resonance. The experimental setup is shown in Fig.9. The $K^-$ beam particles are identified with aerogel Cherenkov detectors and TOF measurement. The outgoing $K^+$ particles are identified by the Kurama spectrometer with aerogel Cherenkov and TOF detectors. The second-level trigger will be introduced to veto protons as in similar previous experiments at KEK and BNL.

The $\Lambda\Lambda$ is produced through the two step reactions; $K^-(p) \rightarrow \pi^0\Lambda, \pi^0(p) \rightarrow K^+\Lambda$ and

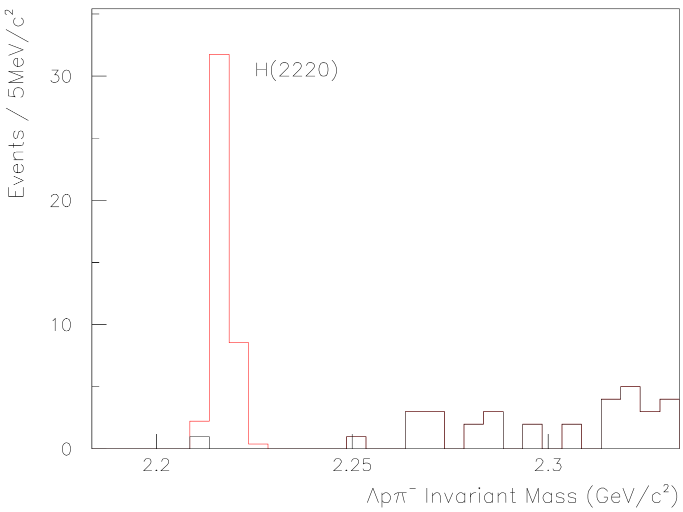


Figure 8: The results of the simulation for the invariant mass spectrum for $\Lambda\pi^-$p decayed from the bound H-dibaryon of 2220 MeV. The production cross section is assumed to be $0.2\mu$b/sr as predicted by A. Aerts and C. Dover.

$K^-(p) \rightarrow K^+\Xi^-, \Xi^-(p) \rightarrow \Lambda\Lambda$. These two-step processes are known to be approximately proportional to $A^{2/3}$ [16]. We employ a Cu target to obtain larger cross section. The target is located at the upstream part of the TPC gas volume to efficiently detect decay particles of hyperons with short flight lengths.

| Parameters | Values |
|---|---|
| $K^-$ beam | $10^6 K^-$ per spill (6 s) |
| Cu target | $4.25 \times 10^{22}$ |
| $d\sigma/d\Omega_L^{Cu}(\Lambda\Lambda)$ | 14.6$\mu$b/sr |
| $\Delta\Omega$ | 0.11 sr |
| Branching ratio ($\Lambda \rightarrow p\pi^-$) | 0.64 |
| Detection efficiency of $K^+$ with Kurama | 0.5 |
| Detection efficiency of two $\Lambda$s with TPC | 0.5 |
| Yield | 0.007 event / spill |

Table 1: Key parameters for yield estimation.

## 2.3 Yield estimation

The estimate of experimental yield for $\Lambda\Lambda$ events has been performed with the following conditions. The $K^-$ beam intensity is assumed to be $10^6$ per spill (in 6 seconds). The Kurama $K^+$ spectrometer is estimated to have a solid angle of 0.11 sr, as listed in Table 1. The $K^+$

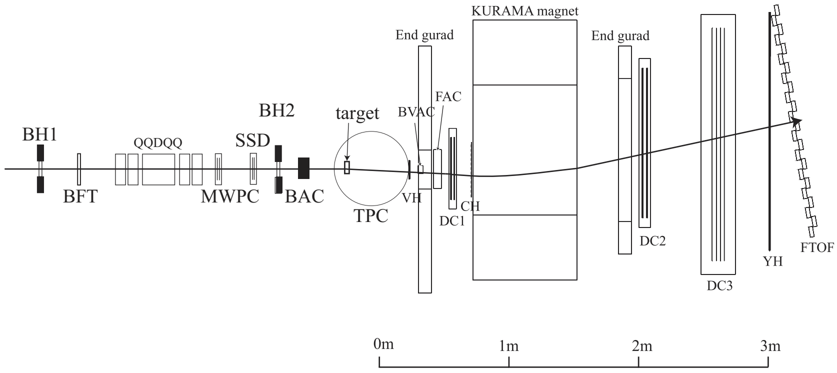


(a)

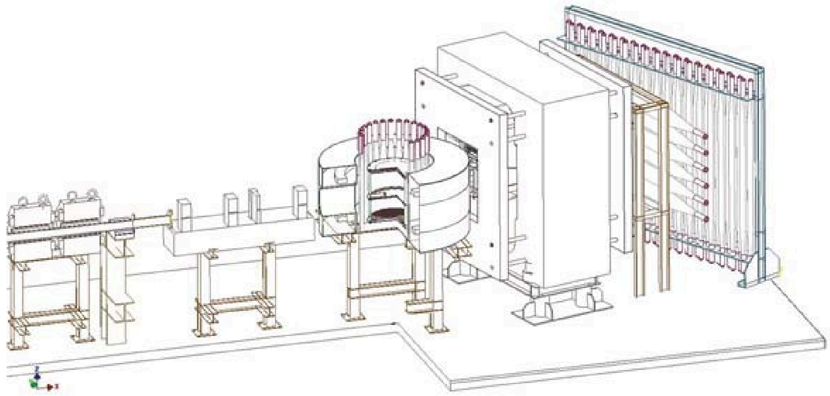

(b)

Figure 9: A schematic view (a) and layout (b) of the experimental setup. The Kurama spectrometer is almost same as the one used in KEK-E522 and written in the correct sizes but the K1.8 beam line spectrometer and the hypTPC spectrometer are only schematically shown.

detection efficiency is assumed to be 0.5, taking in-flight $K^+$ decay probability into account. For a $\Lambda\Lambda$ detection efficiency with TPC, $\Lambda\Lambda$ pairs have been produced in an intra-nuclear cascade calculation, and have been tracked in a cylindrical gas volume of the TPC. In a Geant4 simulation, the minimum track length for charged particles was set to 10 cm, which would leave signals in more than 10 pad layers. The detection efficiency was estimated to reach larger than 0.9 at the target position 10 to 20 cm upstream of the TPC center. However, we take 0.5 as a conservative estimate of the TPC detection efficiency. As a result, we expect to detect 3300 $\Lambda\Lambda$ events in 100 shifts of beam time, which is about 100 times more than those observed in the previous KEK-E224 experiment. If the H-dibaryon cross section is $0.2\mu$b/sr as predicted for $^3$He, the number of the observed H-dibaryons is expected to be about 46 events. For the Cu target, we expect much more events.

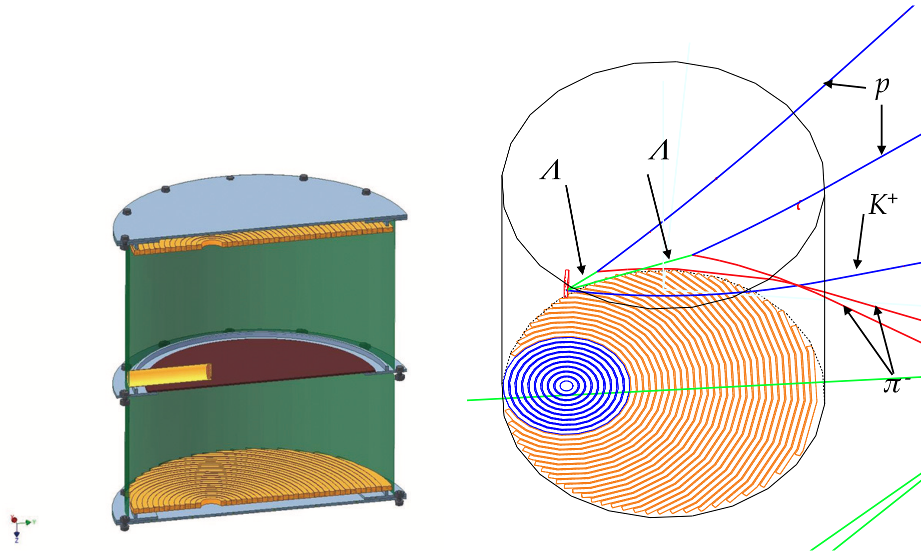

(a) (b)

Figure 10: A schematic view (a) of TPC for HypTPC spectrometer. The target is located inside the TPC. Drifted electrons are amplified through 3 layers of GEM plates and read out with anode pads. A simulated $\Lambda\Lambda$ event is displayed in (b).

## 2.4 Large-acceptance Hyperon spectrometer with TPC (HypTPC)

Two $\Lambda$ particles produced from the Cu target are detected with a large-acceptance hyperon spectrometer. The bound H which decays to $\Lambda p\pi^-$ and $\Sigma^- p$ is also detected with the spectrometer. It consists of a superconducting Helmholtz-type magnet and a TPC (HypTPC).

The TPC is shown schematically in Fig.10a and a typical $\Lambda\Lambda$ event in a Geant4 simulation is displayed in Fig. 10b. In order to efficiently detect low momentum hyperons of which flight length are about a few cm, the target can be located inside the TPC. When $K^+$ particles from $(K^-, K^+)$ reaction at 1.8 GeV$/c$ are tagged at forward angles, $\Xi^-$ and $\Lambda\Lambda$ particles are also predominantly produced in the forward direction. Therefore, the target is located 15 cm upstream of the center of the TPC gas volume.

The superconducting Helmholtz-type magnet is shown in Fig.11a. It provides 1 T magnetic field over a large volume. The calculated magnetic field is shown in Fig.11b. The sensitive field volume about 50 cm in diameter and 50 cm in length has a uniform field within 5%. About 20 cm gap of two coils allows incoming $K^-$ particles and out-going $K^+$ particles detected with the Kurama spectrometer. Both coils are cooled with a compact refrigerator for easy maintenance.

The TPC has a cylindrical configuration to fit with the inner structure of the magnet. The signals are amplified and read with GEM sheets and anode pads at both ends of the TPC. A special care will be taken to provide uniform electric field near the target. (We constructed a

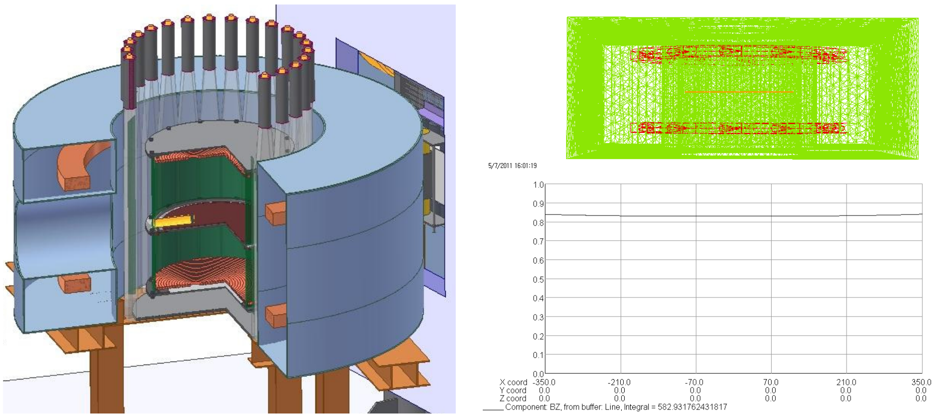


(a) (b)

Figure 11: A schematic view (a) of the Helmholtz-type magnet. Magnetic field strengths along the radial direction at the beam height are displayed in (b), calculated using the OPERA3D.

TPC with a target inside type for SPring-8 LEPS and used it for an experiment successfully [19]. We obtained the position resolution of 300 $\mu$m in x-y plane and 600 $\mu$m in z direction (drift direction)). We expect a similar resolution for the proposed TPC. With a position resolution of 300 $\mu$m the pion momentum resolution of about 1% is expected at 300 MeV$/c$ which is the average pion momentum from $\Lambda$ particles from two $\Lambda$ production.

The TPC is operated under a beam intensity of about $10^6$ $K^-$ per spill. Therefore, a gating grid is employed for the triggered operation of the TPC. The P10 gas will be used for the TPC. Three layers of GEM sheets will be used to obtain the gas amplification of more than $10^4$. The signals from each pad are read through preamplifier-shaper and flash ADC. It is important to test how the TPC can be operated with high intensity beam of $10^6$ $K^-$ per spill. We, therefore, carried out test experiments with a prototype TPC, which is described in Appendix. The TPC could be operated successfully at the beam rate up to $10^7$ Hz. We believe the construction of the proposed hyperon spectrometer with TPC is quite feasible.

# 3 Summary

Recent Lattice QCD calculation, which succeeded to reproduce the nucleon-nucleon potential, has been extended to baryon-baryon interactions in SU$_\mathrm{f}(3)$ symmetry by HAL collaboration. They have shown no repulsive core but attractive potential at a short distance in the baryon-baryon interaction in the SU$_\mathrm{f}(3)$ singlet state, namely H-dibaryon channel. They suggest the H-dibaryon may appear as a weakly bound state or a resonant state near the $\Lambda\Lambda$ threshold. NPLQCD collaboration found the bound H-dibaryon in Lattice QCD calculation without SU$_\mathrm{f}(3)$ symmetry and also suggest the H-dibaryon around the threshold. We propose to search for the H-dibaryon resonance in $\Lambda\Lambda$ production from $(K^-, K^+)$ reactions off nuclei and the bound H-dibaryon by its weak decays to $\Lambda p\pi^-$ and $\Sigma^- p$ to answer the long-standing question about the existence of the H-dibaryon. Being able to simultaneously search below and above threshold is a unique and novel feature of this proposal. For this experiment, we propose to construct a large acceptance hyperon spectrometer with a Time Projection Chamber (TPC), in order to detect $\Lambda$ hyperons and other charged particles with high statistics and an excellent energy resolution. We expect to observe 3300 $\Lambda\Lambda$ events in 100 shifts of beam time with the mass resolution of 1.0 MeV. This spectrometer will also enhance the capability of hadron physics at J-PARC.

# References


[1] R.L. Jaffe, Phys. Rev. Lett. **38** (1977) 195.

[2] T. Sakai, K. Shimizu and K. Yazaki, Prog. Theor. Phys. Suppl. **137** (2000) 121; B. Bassalleck, Nucl. Phys. **A639** (1998) 401.

[3] S. Aoki *et al.* (E176), Prog. Theor. Phys. **85** (1991) 1287.

[4] H. Takahashi *et al.* (E373), Phys. Rev. Lett. **87** (2001) 212502.

[5] J.K. Ahn *et al.* (E224), Phys. Lett. **B444** (1998) 267.

[6] C.J. Yoon *et al.* (E522), Phys. Rev. **C75** (2007) 022201.

[7] N. Ishii, S. Aoki and T. Hatsuda, Phys. Rev. Lett. **99** (2007) 022001.

[8] T. Inoue *et al.* (HAL collaboration), Prog. Theor. Phys. **124** (2010) 591.

[9] T. Inoue *et al.* (HAL collaboration), Phys. Rev. Lett. **106** (2011) 162002.

[10] S.R. Beane *et al.* (NPLQCD collaboration), Phys. Rev. Lett. **106** (2011) 162001.

[11] S.R. Beane *et al.* (NPLQCD collaboration), arXiv:1103.2821v1[hep-lat] (2011).

[12] S. Aoki *et al.* (E176), Phys. Rev. Lett. **65** (1990) 1729. J.K. Ahn *et al.* (E224), Phys. Lett. **B378** (1996) 53; R.W. Stotzer *et al.* (BNL-E836), Phys. Rev. Lett. **78** (1997) 3646. Y. Yamamoto *et al.* (BNL-E885), Phys. Lett. **B478** (2000) 401.

[13] A.T.M. Aerts and C.B. Dover, Phys. Rev. **D28** (1983) 450.

[14] M. Vanhalst, W. Cosyn and J. Ryckebusch, Phys. Rev. **C84** (2011) 031302(R).

[15] Y. Itow, PhD thesis (Kyoto Univ.) unpublished.

[16] T. Iijima *et al.*, Nucl. Phys. **A546** (1992) 588.

[17] The cross section value is estimated based on the data for a carbon target [5] and the A-dependence obtained in ref. 13.

[18] J.F. Donoghue *et al.*, Phys. Rev. **D34** (1986) 3434.

[19] M. Niiyama *et al.* (LEPS collaboration), Phys. Rev. **C78** (2008) 035202.

[20] P.B. Demorest *et al.*, Nature, **467** (2010) 1081.

[21] A.M. Gasparyan, J. Haidenbauer and C. Hanhart, preprint.

[22] P.E. Shanahan, A.W. Thomas and R.D. Young, arXiv:1106.2851v1 (2011).

# APPENDIX

## A-1 Test measurement with a prototype TPC

A prototype TPC with GEM readout was constructed at JAEA. It has three layers of GEM sheets of 10 cm $\times$ 10 cm size and a maximum drift length is about 20 cm. The gate grid enables gate operation of TPC. We have tested with readout pads of different sizes as shown in Fig.12a. The signals were read out through preamplifier-shaper and 40 MHz flash ADC. We have recently performed a test measurement of the TPC with a 400 MeV proton beam up to $10^7$ Hz at RCNP.

The setup of the experiment together with other counters is shown in the Fig.12b. The magnetic field was not applied to the TPC. Two types of gas, P10 and Ar-$CF_4$, were used for the test measurement.

Considering the diffusion of drift electrons without magnetic field, we have taken data mostly with 4 mm width pads. We have performed the test measurement of the TPC at the beam intensity from $10^4$ to $10^7$ Hz. The beam was de-focused to 2 to 3 cm in diameter to simulate the beam size at K1.8 beam line of J-PARC. A typical pulse-height distribution of pads for a 400 MeV proton at $10^6$ Hz is shown in Fig.12c.

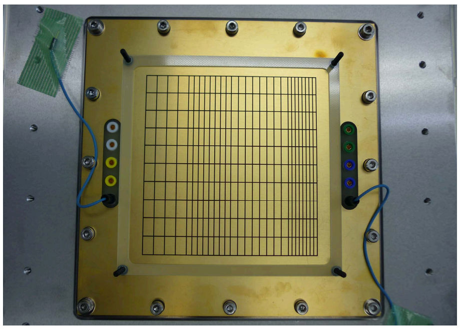

(a)

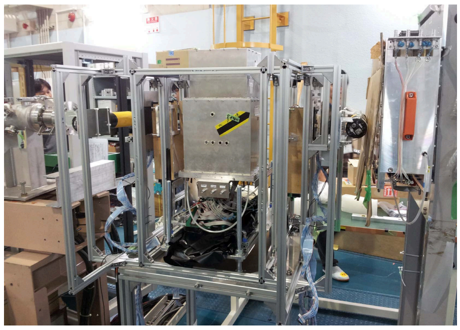

(b)

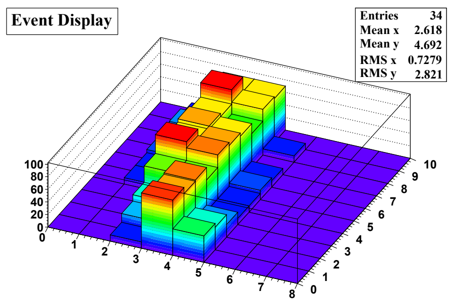


(c)

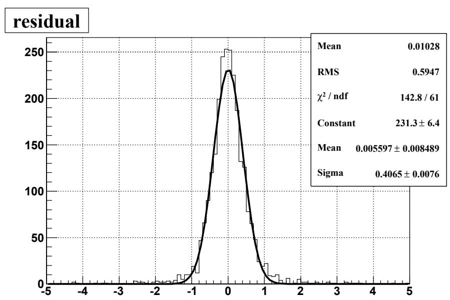


(d)

Figure 12: Cathode pad plane of the prototype TPC (a) and an experimental setup (b) for the beam test are displayed. A typical TPC event is shown in (c) to yield a track residual of 400 $\mu$m in (d).

A track position at each pad row is determined by taking the center of gravity of the pulse-heights for two or three pads in a row. A track is defined as a straight-line fitted to those positions. Fig.12d shows a distribution of the track residual obtained at the beam intensity of $10^6$ Hz with P10 gas. The rms value of the track residual was estimated to be $400\mu$m, which is almost consistent with the pad size and diffusion in the transverse direction without magnetic field. We have not observed any deterioration of the track residual up to $10^6$ Hz of beam intensity, although at $10^7$ Hz it becomes worse in a current simple analysis. The drift velocity for Ar-$CF_4$ gas was about twice faster than that for P10. We found that Ar-$CF_4$ would be appropriate to obtain better two-track separation at high-rate environment. In summary, we have confirmed the TPC can be operated at the beam intensity of $10^6$ Hz.